PCCP

Recovery of enzyme structure and activity following rehydration from ionic liquid

Journal:	*Physical Chemistry Chemical Physics*
Manuscript ID	CP-ART-02-2022-000608.R1
Article Type:	Paper
Date Submitted by the Author:	10-Mar-2022
Complete List of Authors:	Lee, Pei-Yin; University of Maryland at College Park, Chemical Physics Program Singh, Onkar; University of Massachusetts Amherst, Polymer Science and Engineering Bermudez, Harry; University of Massachusetts Amherst, Polymer Science and Engineering Matysiak, Silvina; University of Maryland, Fischell Department of Bioengineering

PCCP

ARTICLE TYPE

Cite this: DOI: 00.0000/xxxxxxxxxx

Recovery of enzyme structure and activity following rehydration from ionic liquid†

Pei-Yin Lee,‡[a] Onkar Singh,‡[b] Harry Bermudez*[b] and Silvina Matysiak*[c]

Received Date
Accepted Date

DOI: 00.0000/xxxxxxxxxx

Long-term preservation of proteins at room temperature continues to be a major challenge. Towards using ionic liquids (ILs) to address this challenge, here we present a combination of experiments and simulations to investigate changes in lysozyme upon rehydration from IL mixtures using two imidazolium-based ILs (1-ethyl-3-methylimidazolium ethylsulfate, [EMIM][$EtSO_4$] and 1-ethyl-3-methylimidazolium diethylphosphate, [EMIM][Et_2PO_4]). Various spectroscopic experiments and molecular dynamics simulations are performed to ascertain the structure and activity of lysozyme. Circular dichroism spectroscopy confirms that lysozyme maintains its secondary structure upon rehydration, even after 295 days. Increasing the IL concentration decreases the activity of lysozyme and is ultimately quenched at sufficiently high IL concentrations, but the rehydration of lysozyme from high IL concentrations completely restores its activity. Such rehydration occurs in the most common lysozyme activity assay, but without careful attention, this effect on the IL concentration can be overlooked. From simulations we observe occupation of [$EMIM^+$] ions near the vicinity of the active site and the ligand-lysozyme complex is less stable in the present of ILs, which result in the reduction of lysozyme activity. Upon rehydration, fast leaving of [$EMIM^+$] is observed and the availability of active site is restored. In addition, suppression of structural fluctuations is also observed when in high IL concentrations, which also explains the decrease of activity. This structure suppression is recovered after undergoing rehydration. The return of native protein structure and activity indicates that after rehydration lysozyme returns to its original state. Our results also suggest a simple route to protein recovery following extended storage.

1 Introduction

A fundamental task of proteins is their activity as enzymes, which are needed to catalyze many biological reactions. Protein denaturation will likely result in the loss of protein catalytic function[1,2]. In addition, blocking of an enzyme's active site by competitive molecules against the natural ligands or changes in protein fluctuations will also affect protein activity. From several literature studies it is reported that the use of ionic liquids (ILs) is a promising technique in protein refolding and stabilization[3–6]. The effect of long-time preservation of proteins in ILs on protein activity is critical in protein-IL pairing design.

Much effort has gone into studying the effects of ILs on protein structure and activity[7–15], but only a few of the literature examples discuss the effects of ILs on proteins after long-time preservation[14,15]. Previous studies have focused on different proteins and ILs, and many observations are protein dependent, or sometimes IL concentration dependent. Yu *et al.* reported the increase in α-helical content of lysozyme in low concentration of imidazolium based ILs leading to more stable structures and no changes in activity. However, the stabilization is reversed to destabilization as the IL concentration increases[9]. A similar finding is also reported by Mogha *et al*[16]. On the other hand, high IL concentration resulting in little loss of activity after solvated in imidazolium ILs is observed with hyperthermophilic enzymes[7] and papain[8].

It has become increasingly common to study protein behaviors in IL-rich solvents[14,17–20]. However, the enzyme concentration is generally held quite low. In case of lysozyme in particular, the most common activity assay is based on turbidity changes due to lysis of *Micrococcus lysodeikticus*. This assay introduces a volume change in the range of *twenty- to thirty-fold*, with a corresponding large effect on the concentrations of the enzyme, and more importantly, the IL. The reported activities of lysozyme in several papers including the works discussed above[9,16,17,19,21] appear to

[a] *Chemical Physics Program, Institute for Physical Science and Technology, University of Maryland, College Park, USA.*
[b] *Department of Polymer Science and Engineering, University of Massachusetts, Amherst, MA, USA. Tel: +1 413 577 1413; E-mail: bermudez@umass.edu*
[c] *Fischell Department of Bioengineering, University of Maryland, College Park, USA. Tel: +1 301 405 0313; E-mail: matysiak@umd.edu*

† Electronic Supplementary Information (ESI) available. See DOI: 10.1039/cXCP00000x/

‡ These authors contributed equally to this work.

not account for these changes in IL concentration, possibly leading to erroneous conclusions regarding the effect of ILs on enzyme activity. Therefore, extra attention has to be paid when looking at the protein activity in ILs.

With experimental observations we learn that different protein-IL combinations will lead to different effects on protein activity, but a systematic rule is still lacking to understand whether the change of activity depends on change of protein stability or the availability of active site. In addition, whether the reduction of activity is reversible or irreversible is not thoroughly discussed in these works. To answer these questions, molecular dynamics is a powerful tool to provide a wealth of detailed atomic-scale structure and microscopic kinetics when inaccessible to experimental techniques. Properties related to protein activity can be examined through simulations and linked back to the activity measured from experiments. Some properties that can be studied by molecular dynamics include the changes in protein conformation, the fluctuation degree of the structure, and the interaction between ILs and the protein, especially with the active site residues.

Previously we have shown that [EMIM][$EtSO_4$] and [EMIM][Et_2PO_4] destabilize lysozyme locally through cation binding to a critical stabilization site and globally through anion effects[22]. Here we study the effects of the same ILs on lysozyme structure and activity before and after rehydration, where lysozyme is preserved in ILs for almost a year. We demonstrate that addition of water, or *rehydration*, has a dramatic impact on both lysozyme structure and activity. Experiments and simulations are combined to complement each other to give a more complete picture on how these ILs affect the protein behavior. We first look at the secondary and tertiary structures of lysozyme before and after rehydration and then study the changes of lysozyme activity before and after rehydration and investigate the possible causes via molecular dynamics simulations.

2 Experimental

2.1 Materials

1-Ethyl-3-methylimidazolium ethylsulfate [EMIM][$EtSO_4$] (>95%), 1-ethyl-3-ethylimidazolium diethylphosphate [EMIM][Et_2PO_4] (>98%), and lysozyme (>90%) from chicken egg white were purchased from Sigma-Aldrich. *Micrococcus lysodeikticus* lyophilized cells were purchased from Worthington biochemical corporation. Potassium phosphate monobasic (>99%) and potassium phosphate dibasic (99.5%) were purchased from Fisher Scientific.

2.2 Sample preparation

Lysozyme solutions (10 wt%) were prepared by dissolving 30 mg of lysozyme in 270 mg of various IL–water (17 to 75 wt%) or buffer (50 mM potassium phosphate, pH 6.2), and stored at room temperature. Lysozyme samples were subsequently rehydrated for circular dichroism, activity assays, and differential scanning calorimetry measurements. For lysozyme samples prepared in phosphate buffer this same buffer was used for rehydrations; for samples prepared in IL-water mixtures, water was used for rehydrations.

2.3 Activity assay

In one activity assay, we followed the manufacturer's instructions (Sigma-Aldrich), based on the lysis of *Micrococcus lysodeikticus*. First, a suspension of *M. lysodeikticus* was prepared at 0.15 mg/ml in 50 mM potassium phosphate buffer, pH 6.2. Stock lysozyme solutions at 10 wt% were diluted to 0.001 wt% (400 units/ml), the recommended concentration, by using phosphate buffer. To begin the activity assay 80 μL of the lysozyme solution were mixed with 2 mL of the *M. lysodeikticus* suspension. Activities were determined by measuring the decrease in turbidity at 450 nm over the initial 5 min at 20°C. Turbidity was recorded on a UV-3600 Shimadzu UV-VIS-NIR spectrophotometer with quartz cuvette having path length of 10 mm.

In another activity assay the aim was to maintain a constant solvent composition. To do so, all samples were separately prepared using identical IL-buffer concentration (e.g., 0.5 – 17 wt%). *Micrococcus lysodeikticus* lyophilized cells were prepared at 0.15 mg/ml and lysozyme solutions were prepared at 0.001 wt% (400 units/ml). To begin the activity assay 80 μL of the lysozyme solution were mixed with 2 mL of the *M. lysodeikticus* suspension. As in the first assay, activities were determined by measuring the decrease in turbidity at 450 nm over the initial 5 min at 20°C. Turbidity was recorded on a UV-3600 Shimadzu UV-VIS-NIR spectrophotometer with quartz cuvette having path length of 10 mm. Both activity assays are schematically depicted in Figure S1.

2.4 Circular dichroism (CD) Spectroscopy

The CD spectra were recorded in the far-UV region (190–260 nm) on a Jasco J-1500 spectrophotometer at 20±1 °C, with a quartz cuvette having path length of 1 mm. Both the data pitch and bandwidth were set to 1 nm with scanning speed of 100 nm/min.

2.5 Differential scanning calorimetry (DSC)

DSC experiments for the samples having 10 wt% lysozyme were carried with a TA Q100 with refrigerated cooling system. Approximately 10 mg of solution was hermetically sealed in an aluminum pan and an empty pan used as a reference. For measuring the unfolding temperature T_m, samples were heated from 20 to 100°C with a heating rate of 2°C/min. The instrument was calibrated using sapphire and indium.

DSC experiments for the samples having 0.1 wt% lysozyme were performed with a MicroCal VP-DSC. All samples were degassed with a MicroCal ThermoVac for 10 minutes before DSC runs. Sample cell reservoir was filled with lysozyme-IL-water solutions while reference cell reservoir was filled with equal volume of IL-water solution. Temperature scans were run from 20 to 100 °C with a scan rate of 90°C/hour, prescan thermostat was set at 5 min and post cycle thermostat was 25°C.

2.6 Simulations

Five systems containing lysozyme (water, 50 wt% [EMIM][$EtSO_4$], 50 wt% [EMIM][Et_2PO_4], rehydrated [EMIM][$EtSO_4$], and rehydrated [EMIM][Et_2PO_4]) were simulated with all-atom molecular dynamics using Gromacs 2018 package[23]. The number of water molecules, IL ions, and

neutralized ions (Cl^-) for each system are provided in Table 1. For the starting protein structure, the coordinates of chicken egg white lysozyme (PDB code ID: 1AKI) was taken with all crystallographical water molecules removed. OPLS-AA force field[24] was used for lysozyme, water and chloride ions. The force field parameters for ILs based on Lopes *et al*[25] and the LigParGen server[26] were taken from our previous work[22]. For the initial conformation of the rehydrated systems, the final conformation of the corresponding 1μs simulation of the 50 wt% system was taken and aligned with the protein crystal structure that is in its ligand-bound form with an oligosaccharide (tri-N-acetylchitotriose) (PDB code ID: 1HEW). All the ILs that are outside of a cutoff (0.6 nm for $[EMIM^+]$ and 0.6 nm for $[EtSO_4]^-$) from any atom of the ligand are removed in the rehydrated $[EMIM][EtSO_4]$ system, leaving only the ILs that are potentially interacting with the active site region. These cutoff values are similar to the shortest distance between the ligand and the active site residues and were thus chosen in order to select a reasonable amount of ILs that aims to mimic the status of the active site when the system is undergoing rehydration. A cutoff of 0.6 nm and 0.52 nm for $[EMIM^+]$ and for $[Et_2PO_4]^-$ were used respectively for the rehydrated $[EMIM][Et_2PO_4]$ system for the same purpose. The reason of different cutoff values for the cation and anion is because by using these cutoff values, the same number of cations and anions can be selected to make the system neutral. Water molecules and neutralized ions were then added to solvate the whole system. The number of water molecules depends on the box size, which has the edge at least 1 nm from the protein and the initially selected ILs. For the rehydrated $[EMIM][EtSO_4]$ system, the final concentration is 0.82 wt%, and for the rehydrated $[EMIM][Et_2PO_4]$ system, the final concentration is 0.73 wt%. The pH of the systems were set at 7 to match experimental conditions of buffer.

	Water	Cation	Anion	Cl^-	df
Water	10636	N/A	N/A	8	N/A
50 wt% $[EMIM][EtSO_4]$	6348	485	485	8	N/A
50 wt% $[EMIM][Et_2PO_4]$	6292	429	429	8	N/A
Rehydrated $[EMIM][EtSO_4]$	12713	8	8	8	60.63
Rehydrated $[EMIM][Et_2PO_4]$	19995	10	10	8	42.90

Table 1 Number of water molecules, IL ions, and chloride ions for each system along with the dilution factors if applicable.

Prior to production runs, the energy of the system was minimized using the steepest descent method, followed by isochoric-isothermal (NVT) and isobaric-isothermal (NPT) ensemble runs of 100 ps each and at 300 K. Pressure for NPT equilibration was set at 1 bar. For the production run, water and 50 wt% systems were run for 1 μs at 300K and the rehydrated systems were run for 500 ns at 300K. Three replicas with different velocity random seeds were performed for the rehydrated systems. All production runs were run with NPT ensemble with a time step of 2 fs and pressure at 1 bar. Linear Constraint Solver Algorithm (LINCS) was used for the constraint algorithm and all bonds involving hydrogens were constrained. The cutoff for both short range Coulomb and van der Waals interactions was 1.0 nm. The particle-mesh Ewald method[27] was used for the long-range electrostatic interactions. Parrinello-Rahman barostat[28] and V-rescale thermostat were used to control pressure and temperature, respectively.

The last 500 ns data of water and 50 wt% systems and the whole 500 ns trajectories for the rehydrated systems were used for the analysis. For the spatial distribution function (SDF) figures, isovalues of 0.015051 and -0.014899 were used for $[EMIM^+]$ in the 50 wt% $[EMIM][EtSO_4]$ system and 50 wt% $[EMIM][Et_2PO_4]$ system, respectively. For the $[EMIM^+]$ time series analysis, the cutoff of the $[EMIM^+]$ near active site is the same as that was used to construct the initial rehydrated system. All other analyses along with SDF were done with the inbuilt tools in Gromacs or VMD[29]. All structure images were rendered from VMD.

A set of umbrella sampling simulations were performed in water and in 50 wt% $[EMIM][EtSO_4]$. The topology and the OPLS-AA force field parameters for the sugar ligand (tri-N-acetylchitotriose) were generated with the LigParGen server and relaxed through energy minimization and a short NPT equilibration. The equilibrated ligand was then combined with the lysozyme structure (1AKI.pdb) with the same protein-ligand alignment as that in the lysozyme-ligand complex (1HEW.pdb). The lysozyme-ligand complex was then put into a 6.3 nm * 6.3 nm * 13 nm box. The box was then solvated with water and neutralized with 8 chloride ions. The complex system went through a set of energy minimization and NPT equilibration (time step 2 fs for 100 ps). The pulling simulation was then conducted with a pulling rate of 0.01 nm/ps. The center of mass (COM) of the ligand was pulled away from the COM of lysozyme along the direction of the principal axis of the ligand. A total of 30 conformations were saved for the following umbrella sampling simulations. Conformations with different lysozyme-ligand distance were first equilibrated with NPT (time step 2 fs for 100 ps) and then the production run (time step 2 fs for 30 ns). Weighted histogram analysis method (WHAM), a built-in tool in Gromacs, was applied to extract the potential mean force (PMF) from various umbrella sampling runs and the free energy landscape along a reaction coordinate (distance between the COM of the ligand and the COM of lysozyme) was then generated.

3 Results and Discussion

To test the ability of ILs to preserve lysozyme over time, this protein was dissolved in various IL-water mixtures and maintained at room temperature. At selected times, aliquots were taken and rehydrated to different extents by the addition of water (or buffer in the case of control samples). The extent of rehydration is given by the "dilution factor" df, i.e., the ratio of final to initial volume.

3.1 Lysozyme secondary structure is preserved after rehydration

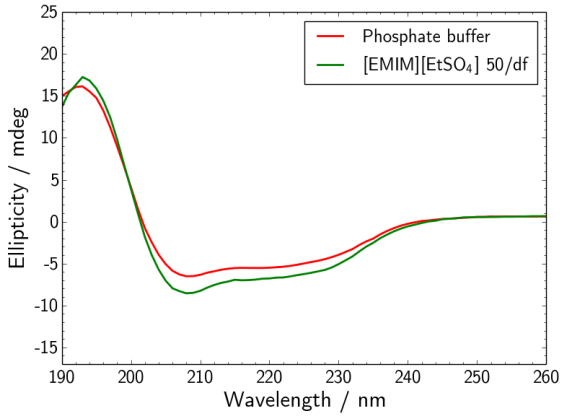

Fig. 1 Far-UV CD spectra of lysozyme. Freshly prepared sample in phosphate buffer (red), freshly prepared in 50 wt% [EMIM][$EtSO_4$] and rehydrated with water (green). The dilution factor df = 1000.

To probe the secondary structure of lysozyme, we used far-UV circular dichroism (Figure 1). We find that lysozyme maintains its secondary structure after rehydration from high IL content, showing characteristic features near 210 and 230 nm[30]. Prior to rehydration, circular dichroism cannot be performed at high IL content due to absorbance by the imidazolium cation[31]. Nevertheless from the CD data we deduce two possibilities, either: (i) lysozyme structure is preserved in high IL content before rehydration, or (ii) lysozyme structure is perturbed in high IL content but is recovered after rehydration. However, *simulations are uniquely able to examine the protein both before and after.*

In order to study computationally the possible changes in structure fluctuation and conformation of lysozyme before and after rehydration, root mean squared fluctuation (RMSF) and the average structure over a 500 ns time course are computed. Figure 2a and 2b show the RMSF of lysozyme in water, 50 wt% and rehydrated systems for [EMIM][$EtSO_4$] and [EMIM][Et_2PO_4], respectively. The RMSF for both 50 wt% IL systems are in general more suppressed compared to that in water, possibly due to high density regions of ILs on the protein surface reducing the conformational freedom as shown in our previous publication[22]. This dampening of dynamics motion by ILs has also observed for family 11 xylanase in [$EMIM^+$] based ILs[32]. In addition, the suppression of structure fluctuation is more obvious for [EMIM][Et_2PO_4] than for [EMIM][$EtSO_4$], which could be explained by the stronger electrostatic interaction between the [Et_2PO_4] and the protein surface as indicated by our previous work.

After rehydration, the RMSF of both rehydrated systems are recovered to be close to the values in water. There are three regions with particularly high RMSF values (region I: residue 45 - 51; region II: residue 64 - 75; region III: residue 99 - 127). Region I and II correspond to the loops, with region I being near to the active site residues as shown in Figure 3. Region III contains some small helical fragments, but is mostly coil and is located at the C-terminus. Other regions that do not show high RMSF values are either buried or well structured (for example, a structured α helix). The reason why the RMSF values of region II and region III for the rehydrated [EMIM][Et_2PO_4] system are not fully recovered back to the values in water could be explained by the high B factors of lysozyme in these regions (Figure 2c), where a high B factor indicates a higher flexibility of the residue. The high flexibility in residue could possibly lead to a larger deviation in the RMSF values. In addition, one might wonder if the lower RMSF values of region II and III in rehydrated [EMIM][Et_2PO_4] could come from ILs having interactions with these loop regions that might cause the slight suppression. In order to answer this question, the trajectory of the rehydrated [EMIM][Et_2PO_4] system is examined with a focus on these two regions, and no specific binding of ILs is observed for both loops (results not shown).

In Figure 3, the average structures in water, 50 wt% and rehydrated systems are aligned. It is observed that region I in water and in rehydrated system are nicely overlapped in both IL systems, even though the RMSF is not fully recovered. On the other hand, region I of 50 wt% ILs deviates from that in water and in rehydrated system. In 50 wt% [EMIM][Et_2PO_4], this deviation in region I is even more obvious. For the 50 wt% systems, although the overall tertiary structures are preserved as well as the secondary structures, the suppression of loop fluctuations and the deviation of region I could possibly affect the activity of lysozyme, considering the close proximity of region I and the active site residues.

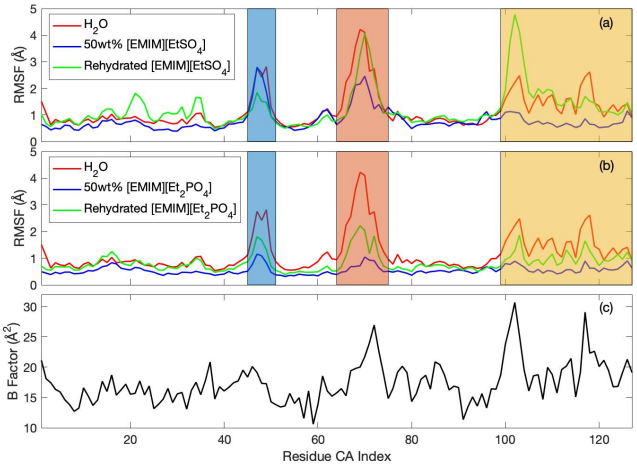

Fig. 2 RMSF of water (red), 50 wt% ILs (blue) and rehydrated (green) systems for (a) [EMIM][$EtSO_4$] and (b) [EMIM][Et_2PO_4]. Blue: Region I; Orange: Region II; Yellow: Region III. (c) is the B factor recorded in 1AKI.pdb.

3.2 Lysozyme activity is restored after rehydration

To determine the functional capabilities of lysozyme, we measured enzymatic activity using a well-known turbidity assay[33]. Following the manufacturer's instructions corresponds to a dilution factor df = 26, and we realized that this large change in solvent environment may explain literature reporting on "increased protein activity in the presence of all ionic liquids examined"[17], among similar results[9,16,19,21]. In our case this dilution was even more significant because of the high lysozyme content,

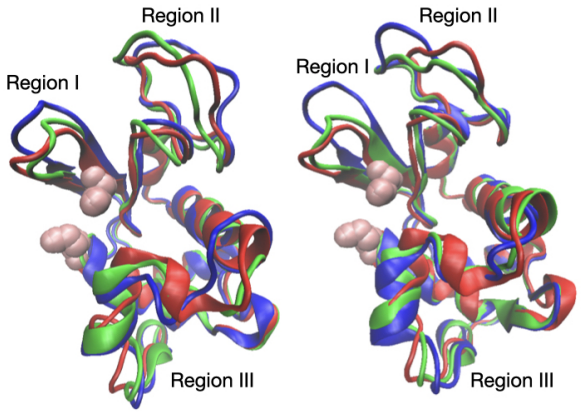

Fig. 3 The alignment of the average structures from water (red), 50 wt% ILs (blue) and rehydrated (green) systems in [EMIM][$EtSO_4$] (left) and [EMIM][Et_2PO_4] (right). Pink vdW representations are the active site residues (residue 35 and 52). The high RMSF regions are also indicated.

such that an additional dilution was needed to bring the lysozyme concentration to the suggested 400 units/mL, for an overall df $= 2.6 \times 10^5$. Nevertheless with this typical activity assay and its corresponding rehydration, activity values similar to controls are obtained (Table 2). Therefore lysozyme activity is *recovered* upon sufficient rehydration with water, but we remained curious as to the effect of the IL on activity.

	[EMIM][$EtSO_4$]	[EMIM][Et_2PO_4]
IL conc., wt%	activity, %	activity, %
$17/df = 6.5 \times 10^{-5}$	115	110
$33/df = 1.3 \times 10^{-4}$	116	98
$50/df = 1.9 \times 10^{-4}$	114	87

Table 2 Normalized lysozyme activity using the typical activity assay, under different conditions. Prior to rehydration all samples here showed no detectable activity, i.e., activity $= 0\%$. The dilution factor df $= 2.6 \times 10^5$.

To address the effect of the IL on activity more directly, we performed a separate activity assay where the IL content was maintained at a constant level throughout the assay. With this modified activity assay, there is a *complete absence* of lysozyme activity at even moderate IL levels (greater than or equal to 10 wt%). Figure 4 shows a steep change in activity as [EMIM][$EtSO_4$] is increased, with the 50% activity level corresponding to approximately 3 wt% IL. Similar results were obtained for [EMIM][Et_2PO_4], with the 50% activity level corresponding to approximately 5 wt% IL (data not shown). In short, the activity $= 0\%$ in the presence of sufficient IL. This result is presumably due to blocking of the active site, as interpreted from simulation results that correspond to approximately 1 wt% IL, where the lysozyme activity is fully recovered (see below). The concentration of ILs before rehdyration for simulations is 50 wt%, which is on the right side of the sigmoidal curve, showing no activity.

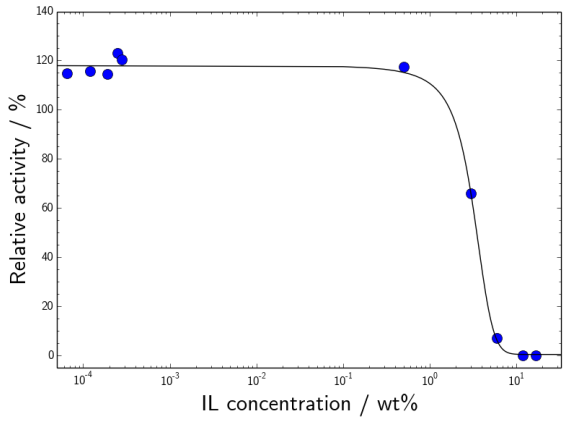

Fig. 4 Normalized lysozyme activity as a function of [EMIM][$EtSO_4$] content using a modified activity assay to avoid dilution steps. The curve fit is a Boltzmann-type sigmodial function.

In a separate set of experiments with samples aged more than 1 year in IL-water mixtures, lysozyme activity can be restored to greater than 75% relative to control samples (Figure S2), irrespective of the initial IL content. Therefore the presence of these two imidazolium ionic liquids, even after prolonged incubation, can be easily displaced by water and the lysozyme activity recovered.

To gain a molecular understanding on the reduction of lysozyme activity in the presence of 50 wt% ILs, we first computed the average lysozyme structures in 50 wt% ILs and aligned them with the crystal structure of the lysozyme-ligand complex (1HEW.pdb). In Figure 5, the orange van der Waals (vdW) representations correspond to the lysozyme active site residues (Glu35 and Asp52) while the yellow vdW representations correspond to Trp62 and Trp63. The non-native sugar ligand is shown in green. In addition, the SDF of [$EMIM^+$] is expressed in red. Although the IL concentrations are quite high, unlike water as a solvent that is homogeneously distributed around the protein, ILs show specific patching to the lysozyme surface. From the SDF we observe a clear overlapping between the sugar ligand and a high density region of [$EMIM^+$] in both systems. The sugar ligand is clamped by Trp62 and Trp63 as illustrated. These two aromatic residues also interact with [$EMIM^+$] ions as seen from the high [$EMIM^+$] density nearby. Other than the overlapping at the non-native ligand position, [$EMIM^+$] also occupies the vicinity of the active site (see [$EMIM^+$] distribution between Trp62/63 and the active site residues and as pointed by the green arrows in Figure 5). The occupation of [$EMIM^+$] at the ligand position near the active site could compete with the natural ligands and lead to competitive inhibition.

Figure 6 shows the potential of mean force $\Delta G(r)$ for the ligand, where r is the distance of the ligand from the lysozyme active site along the pulling direction. The free energy barrier $\Delta G(r)^{TS}$ for the ligand to leave lysozyme is around 47 kJ/mol in water and 18 kJ/mol in 50 wt% [EMIM][$EtSO_4$], which indicates that it takes less energy for the ligand to leave the active site in ILs. Using transition state theory $k \approx \exp(-\Delta G(r)^{TS}/k_B T)$ where k_B is the Boltzmann constant and T is the temperature, a smaller $\Delta G(r)^{TS}$ would translate into faster unbinding kinetics for 50 wt%

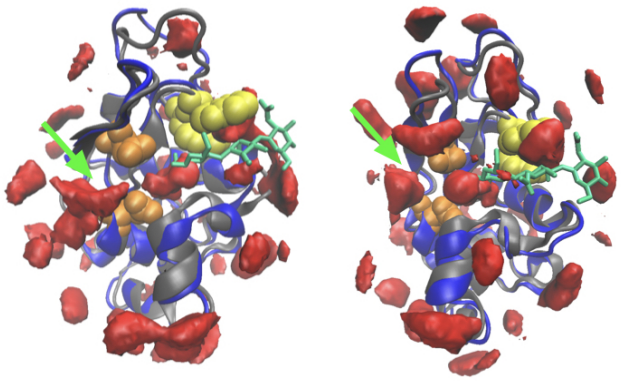

Fig. 5 Overlapping of the lysozyme-ligand complex with the average structure of lysozyme in 50 wt% [EMIM][$EtSO_4$] (left) and [EMIM][Et_2PO_4] (right). In both figures, the crystal structures are in gray, the average structures from simulations are in blue, active site residues are in orange vdW, TRP62/63 are in yellow vdW, non-native sugar ligand is in green vdW and [$EMIM^+$] is in red SDF. The green arrows indicate another region near the active site that is also occupied by high [$EMIM^+$] density.

[EMIM][$EtSO_4$] compared to water. The unbinding free energy in water is around 44 kJ/mol and in 50 wt% [EMIM][$EtSO_4$] is 11 kJ/mol, indicating the protein-ligand complex is less stable in the presence of ILs. We have also calculated the potential energy of the ligand in the active site and in the bulk solvent for both water and 50 wt% [EMIM][$EtSO_4$] systems. The difference of ligand potential energy when in the active site and in bulk is similar in the two systems (26.63 kJ/mol in water and 27.93 kJ/mol in IL). Therefore, the lower stability for ligand in IL is driven by a larger entropic gain of the ligand in the bulk IL aqueous mixture. [$EMIM^+$] ions interacting with TRP62/63 and the active site residues could also be a reason why ligand binding is less stable in ILs and explain the dramatic reduction of lysozyme activity observed in experiments when in high IL concentrations.

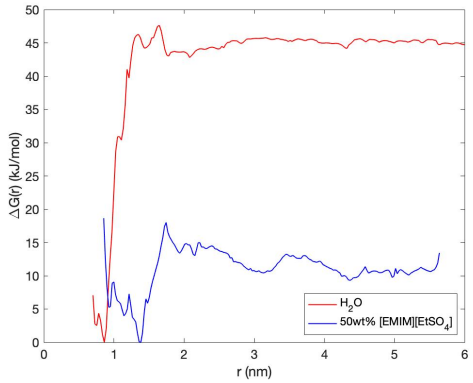

Fig. 6 Free energy profile ΔG(r) of ligand in water (red) and 50 wt% [EMIM][$EtSO_4$] (blue) for moving the ligand away from the lysozyme active site in the pulling direction.

Next we examine the behavior of [$EMIM^+$] ions when undergoing rehydration. Figure 7 shows the time series of the [$EMIM^+$] ions near the non-native ligand binding site in both 50 wt% and rehydrated IL systems. In the 50 wt% IL systems, although the number of [$EMIM^+$] fluctuates, in average there are around two [$EMIM^+$] ions near the ligand binding position. However, for the rehydrated systems, within the first 50 ns, the number of [$EMIM^+$] already decreases to one or two ions in both IL systems. After approximately 200 ns the number of [$EMIM^+$] oscillates between 0 and 1. Two other replicas for the rehydrated system for each IL are performed and from all replicas the fast leaving of [$EMIM^+$] is observed. The diffusion of the [$EMIM^+$] ions indicates that the interactions between [$EMIM^+$] and the neighborhood of the ligand position are not strong enough to keep the [$EMIM^+$] ions from leaving the active site in the rehydrated conditions. Figure S4 also presents the potential of mean force ΔG(r) for an [$EMIM^+$] ion in the active site, where r is the distance of the [$EMIM^+$] ion from the lysozyme active site along the pulling direction in a hydrated system. [$EMIM^+$] ions have a lower free energy in the bulk solution comparing to that in the active site explaining the leaving of the cations.

The re-entrance of the [$EMIM^+$] ion into the ligand binding region after 200 ns is not because of the narrow selection of the cutoff. The rehydrated systems for both ILs are very dilute (less than 1 wt%) and [$EMIM^+$] can diffuse far away from lysozyme. There is no specificity of this one ion, different [$EMIM^+$] ion enters the active site region and leaves. The re-entrance of [$EMIM^+$] ions interact with the active site residues (Figure S4a) or TRP62/63 (Figure S4b). The interaction between [$EMIM^+$] and active site residues are mainly electrostatic, while the interaction between [$EMIM^+$] and TRP62/63 could be cation-π and hydrophobic effects. However, the re-entrance of the cations is quite short-lived. The fast leaving of [$EMIM^+$] ions could explain why after rehydration the lysozyme activity can be fully recovered in experiments [$EMIM^+$].

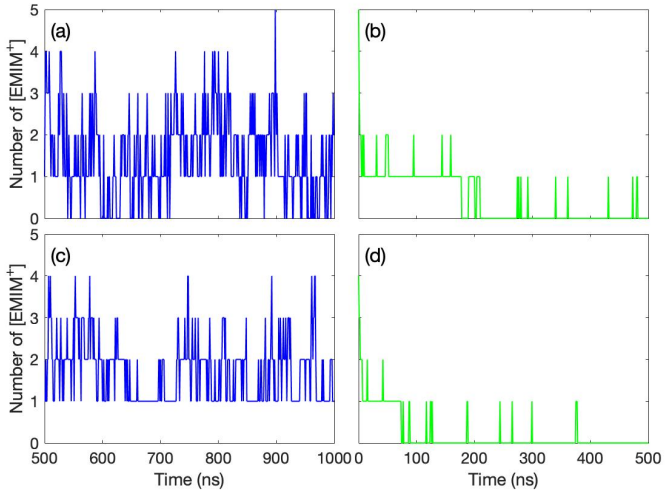

Fig. 7 The time series showing the number of [$EMIM^+$] ions near the non-native ligand binding site, where (a) is the 50 wt% [EMIM][$EtSO_4$] system, (b) is the rehydrated [EMIM][$EtSO_4$] system, (c) is the 50 wt% [EMIM][Et_2PO_4] system, and (d) is the rehydrated [EMIM][Et_2PO_4] system.

The results here point to a robust behavior for lysozyme in

these two imidazolium ionic liquids. Part of this behavior can be explained by the unusually high stability of lysozyme itself, which has been known for decades[34]. Both ILs have different interaction strengths with lysozyme, with [EMIM][$EtSO_4$] being the weaker of the two. As a consequence this IL perturbs lysozyme structure, and activity, to a smaller degree. Nevertheless, with the addition of sufficient water the protein's enzymatic activity is almost completely restored.

3.3 T_m returns to initial value after rehydration

	lysozyme 10 wt%		lysozyme 10/df wt%	
	IL conc., wt%	T_m, °C	IL conc., wt%	T_m, °C
Buffer	0	75.3[a]	0	74.6[b]
[EMIM][$EtSO_4$]	50	58.1[a]	50/df	75.9[b]
[EMIM][Et_2PO_4]	33	59.9[a]	33/df	75.3[b]

Table 3 Lysozyme melting temperature T_m under different conditions. All samples here are aged in their respective solvents for more than 1 year. The dilution factor df = 100. [a] DSC. [b] VP-DSC.

Previous works by our group[22] and others[12,35] have shown variation of the lysozyme melting temperature T_m in an IL-dependent manner. Here we find that even when T_m is reduced by the ILs, it remains far above room temperature (Table 3), indicating that a large majority of the lysozyme protein is still in its native folded state when in presence of these ILs at room temperature. With the addition of a relatively modest amount of water (df = 100), the T_m return to their original values (Table 3). From the combined experimental and simulation results we suggest that the process observed here is *not refolding*, but rather a rehydration that returns lysozyme to its native solvation state. Part of the reason for this behavior is because of the unusually high stability of lysozyme[34].

4 Conclusions

Circular dichroism data and simulations both show that lysozyme structure is preserved after rehydration from high IL content, even after prolonged storage times (i.e., approaching one year). From the RMSF analysis, the suppressed protein structure fluctuations in 50 wt% ILs are able to recover back to higher fluctuations after rehydration. In addition, the average structure analysis also shows the deviation of the region I position from the aqueous structure (close to the active site) in 50 wt% ILs, and this deviation is able to restore back in the rehydrated systems. This is an important finding given the current interest in IL-based storage media to "break the cold chain" for protein therapeutics[36].

Activity data and simulations both show that lysozyme's enzymatic function is suppressed at high IL content but is recovered upon sufficient rehydration with water. From simulations it is observed that [$EMIM^+$] ions occupying the ligand position and the vicinity of the active site. The ligand-lysozyme complex in 50 wt% [EMIM][$EtSO_4$] has lower binding-unbinding energy than that in water as shown by umbrella sampling simulations, indicating that the ligand-lysozyme complex is less stable in the presence of ILs. These results explain the reduction of lysozyme activity when in high IL content. The presence of [$EMIM^+$] near the active site leading to loss of protein activity agrees with several other works that concern different protein/ILs systems[32,37]. When undergoing rehydration, the fast leaving of [$EMIM^+$] ions is observed for both IL systems, which explains the reappearance of the active site availability because there is no more cations present near the active site after rehydration. This result verifies the concept of recovering functional proteins from IL media.

Conflicts of interest

There are no conflicts to declare.

Acknowledgements

We acknowledge financial support from the National Science Foundation (CBET-1760879 for PL and SM and CBET-1800442 for OS and HB).

Notes and references

1 V. V. Mozhaev, Y. L. Khmelnitsky, M. V. Sergeeva, A. B. Belova, N. L. Klyachko, A. V. Levashov, and K. Martinek, *European Journal of Biochemistry*, 1989, **184**(3), 597–602.

2 M. Arroyo, R. Torres, I. de la Mata, M. P. Castillón, and C. Acebal, *Enzyme and microbial technology*, 1999, **25**(3-5), 378–383.

3 D. K. Sasmal, T. Mondal, S. Sen Mojumdar, A. Choudhury, R. Banerjee, and K. Bhattacharyya, *The Journal of Physical Chemistry B*, 2011, **115**(44), 13075–13083.

4 U. K. Singh, M. Kumari, F. A. Wani, M. ud din Parray, J. Saraswat, P. Venkatesu, and R. Patel, *Colloids and Surfaces A: Physicochemical and Engineering Aspects*, 2019, **582**, 123872.

5 H. Weingärtner, C. Cabrele, and C. Herrmann, *Physical Chemistry Chemical Physics*, 2012, **14**(2), 415–426.

6 P. Attri and P. Venkatesu, *Physical Chemistry Chemical Physics*, 2011, **13**(14), 6566–6575.

7 S. Datta, B. Holmes, J. I. Park, Z. Chen, D. C. Dibble, M. Hadi, H. W. Blanch, B. A. Simmons, and R. Sapra, *Green Chemistry*, 2010, **12**(2), 338–345.

8 W.-Y. Lou, M.-H. Zong, T. J. Smith, H. Wu, and J.-F. Wang, *Green Chemistry*, 2006, **8**(6), 509–512.

9 X. Yu, N. Tian, F. Huang, X. Huang, C. Liu, S. Gao, Z. Yang, and Y. Wu, *Journal of Molecular Liquids*, 2019, **296**, 112018.

10 L.-P. Dang, W.-Z. Fang, Y. Li, Q. Wang, H.-Z. Xiao, and Z.-Z. Wang, *Applied biochemistry and biotechnology*, 2013, **169**(1), 290–300.

11 D. Constatinescu, C. Herrmann, and H. Weingärtner, *Physical Chemistry Chemical Physics*, 2010, **12**(8), 1756–1763.

12 J. V. Rodrigues, V. Prosinecki, I. Marrucho, L. P. N. Rebelo, and C. M. Gomes, *Physical Chemistry Chemical Physics*, 2011, **13**(30), 13614–13616.

13 A. M. Figueiredo, J. Sardinha, G. R. Moore, and E. J. Cabrita, *Physical Chemistry Chemical Physics*, 2013, **15**(45), 19632–19643.

14 N. Byrne, L.-M. Wang, J.-P. Belieres, and C. A. Angell, *Chemical Communications*, 2007, (26), 2714–6.

15 K. Tonova, *Green Processing and Synthesis*, 2018, **7**(2), 106–113.

16 N. K. Mogha, N. Yadav, A. Sindhu, and P. Venkatesu, *New Journal of Chemistry*, 2019, **43**(42), 16759–16766.

17 J. P. Mann, A. McCluskey, and R. Atkin, *Green Chemistry*, 2009, **11**(6), 785.

18 T. Takekiyo, K. Yamazaki, E. Yamaguchi, H. Abe, and Y. Yoshimura, *Journal of Physical Chemistry B*, 2012, **116**(36), 11092–7.

19 K. D. Weaver, R. M. Vrikkis, M. P. Van Vorst, J. Trullinger, R. Vijayaraghavan, D. M. Foureau, I. H. McKillop, D. R. MacFarlane, J. K. Krueger, and G. D. Elliott, *Physical Chemistry Chemical Physics*, 2012, **14**(2), 790–801.

20 S. H. Strassburg, H. Bermudez, and D. A. Hoagland, *Biomacromolecules*, 2016, **17**(6), 2233–2239.

21 E. C. Wijaya, F. Separovic, C. J. Drummond, and T. L. Greaves, *Physical Chemistry Chemical Physics*, 2016, **18**(37), 25926–25936.

22 O. Singh, P.-Y. Lee, S. Matysiak, and H. Bermudez, *Physical Chemistry Chemical Physics*, 2020, **22**(35), 19779–19786.

23 B. Hess, C. Kutzner, D. Van Der Spoel, and E. Lindahl, *Journal of chemical theory and computation*, 2008, **4**(3), 435–447.

24 W. L. Jorgensen, D. S. Maxwell, and J. Tirado-Rives, *Journal of the American Chemical Society*, 1996, **118**(45), 11225–11236.

25 J. N. Canongia Lopes, A. A. Pádua, and K. Shimizu, *The Journal of Physical Chemistry B*, 2008, **112**(16), 5039–5046.

26 L. S. Dodda, I. Cabeza de Vaca, J. Tirado-Rives, and W. L. Jorgensen, *Nucleic acids research*, 2017, **45**(W1), W331–W336.

27 T. Darden, D. York, and L. Pedersen, *The Journal of chemical physics*, 1993, **98**(12), 10089–10092.

28 M. Parrinello and A. Rahman, *Journal of Applied physics*, 1981, **52**(12), 7182–7190.

29 W. Humphrey, A. Dalke, and K. Schulten, *Journal of Molecular Graphics*, 1996, **14**, 33–38.

30 F. Tanaka, L. S. Forster, P. K. Pal, and J. A. Rupley, *Journal of Biological Chemistry*, 1975, **250**(17), 6977–6982.

31 P. Attri, P. Venkatesu, and A. Kumar, *Physical Chemistry Chemical Physics*, 2011, **13**(7), 2788–96.

32 V. W. Jaeger and J. Pfaendtner, *ACS chemical biology*, 2013, **8**(6), 1179–1186.

33 D. Shugar, *Biochimica et Biophysica Acta*, 1952, **8**, 302–309.

34 K. Hamaguchi, *The Journal of Biochemistry*, 1957, **44**(11), 695–706.

35 R. Buchfink, A. Tischer, G. Patil, R. Rudolph, and C. Lange, *Journal of Biotechnology*, 2010, **150**(1), 64–72.

36 L. Bui-Le, A. P. Brogan, and J. P. Hallett, *Biotechnology and Bioengineering*, 2021, **118**(2), 592–600.

37 S. R. Summers, K. G. Sprenger, J. Pfaendtner, J. Marchant, M. F. Summers, and J. L. Kaar, *The Journal of Physical Chemistry B*, 2017, **121**(48), 10793–10803.